Insights into the Supercritical CO2 Extraction of Perilla Oil and Its Theoretical Solubility

Authors:

Ming-Chi Wei, Chia-Sui Wang, Da-Hsiang Wei, Yu-Chiao Yang

Abstract:

In the current research, the supercritical carbon dioxide (SCCO2) procedure was used to extract volatile oils from perilla leaves. The yields of the volatile oils and the four main constituents, limonene, perillaldehyde, ?-caryophyllene, and (Z,E)-?-farnesene obtained by the SCCO2 procedure were 1.31-, 1.12-, 1.04-, 1.05-, and 1.07-fold higher than those obtained by the hydrodistillation technique, respectively. Furthermore, the duration and temperature of extraction were 40 min and 45 °C lower, respectively, in the former procedure compared to the latter technique. These advantages reveal that SCCO2 not only obtains high-quality extracts, but also meets the requirements of green environmental protection. The theoretical solubilities of the volatile oils acquired by the SCCO2 dynamic extraction at various temperatures and pressures were $1.385 \times 10?3?8.971 \times 10?3$ (g oil/g CO2). Moreover, the three density-based models were well correlated with these theoretical solubility data, with a high coefficient of determination and low average absolute relative deviation.

Insights into the Supercritical CO$_2$ Extraction of Perilla Oil and Its Theoretical Solubility

Ming-Chi Wei [1], Chia-Sui Wang [1], Da-Hsiang Wei [2] and Yu-Chiao Yang [2,3,*]

[1] Department of Environmental Engineering & Science, Chia Nan University of Pharmacy and Science, Tainan 71710, Taiwan; s120702@mail.cnu.edu.tw (M.-C.W.); box1025@mail.cnu.edu.tw (C.-S.W.)

[2] Department and Graduate Institute of Pharmacology, Kaohsiung Medical University, Kaohsiung 80708, Taiwan; dxwei8888@gmail.com

[3] Department of Medical Research, Kaohsiung Medical University Hospital, Kaohsiung 80708, Taiwan

[*] Correspondence: ycyang@kmu.edu.tw; Tel.: +886-7-3121101 (ext. 2139 & ext. 13)

Abstract: In the current research, the supercritical carbon dioxide ($_{sc}CO_2$) procedure was used to extract volatile oils from perilla leaves. The yields of the volatile oils and the four main constituents, limonene, perillaldehyde, β-caryophyllene, and (Z,E)-α-farnesene obtained by the $_{sc}CO_2$ procedure were 1.31-, 1.12-, 1.04-, 1.05-, and 1.07-fold higher than those obtained by the hydrodistillation technique, respectively. Furthermore, the duration and temperature of extraction were 40 min and 45 °C lower, respectively, in the former procedure compared to the latter technique. These advantages reveal that $_{sc}CO_2$ not only obtains high-quality extracts, but also meets the requirements of green environmental protection. The theoretical solubilities of the volatile oils acquired by the $_{sc}CO_2$ dynamic extraction at various temperatures and pressures were 1.385×10^{-3}–8.971×10^{-3} (g oil/g CO_2). Moreover, the three density-based models were well correlated with these theoretical solubility data, with a high coefficient of determination and low average absolute relative deviation.

Keywords: *Perilla frutescens*; hydrodistillation; supercritical carbon dioxide extraction; essential oils; perillaldehyde; density-based models

1. Introduction

Perilla frutescens (L.) Britton is a famous edible and medicinal plant that belongs to the Lamiaceae family [1,2]. Due to its special flavor, perilla leaves have a special flavor, they are often eaten directly as fresh vegetables or used as food additive material or in sushi. Furthermore, perilla leaves are a widely used traditional medicinal material because of their rich and diverse pharmacological properties, such as anticancer, antioxidative, neuroprotective, anti-inflammatory, and antimicrobial activities [2–4]. Essential oil has been reported to be an important bioactive ingredient in perilla leaves [5]. Perilla essential oil is not only used as a food and nutritional additive, but also has been extensively researched for its anticancer, antioxidative, neuroprotective, anti-inflammatory, and antimicrobial effects [3,6]. The chemical composition of perilla essential oil varies according to the variety, geographical factors, climatic conditions, and planting and harvest times. However, for red-leafed varieties of *P. frutescens*, the main volatile component has been found to be perillaldehyde [3,6]. Gas chromatography was used to study essential oils obtained from perilla leaves, providing qualitative and quantitative analyses with sufficient accuracy for the aforementioned components [5].

Hydrodistillation (HD) and steam distillation (STD) have been widely used to separate essential oils from *P. frutescens* because of the use of water as the solvent and simple operation [7–9]. However, these traditional procedures require the use of high temperatures; they often cause the degradation of heat-sensitive ingredients, thus affecting the quality of essential oils. Moreover, the procedures often cause the mixing of water-soluble components and essential oils, and further separation procedures cause the loss of essential

oils. However, the long extraction time is the most frequently criticized drawback of these traditional procedures.

Because of the unique properties of supercritical carbon dioxide ($_{SC}CO_2$), such as a low critical point (7.4 MPa, 31.1 °C), chemical inertness, and high penetration and diffusion capabilities, $_{SC}CO_2$ extraction can perfectly solve the shortcomings of traditional procedures [10]. This is mainly due to the low critical point of CO_2, it does not need a very high temperature to achieve good extraction results, so it does not cause degradation of heat-sensitive components. Additionally, $_{SC}CO_2$ does not react with the constituents of the extract, so the $_{SC}CO_2$ procedure obtains a highly stable extract. Furthermore, after the extraction process is decompressed, CO_2 and the extract can be completely separated, so there is no concern about solvent residue in the extract. Based on the abovementioned advantages, $_{SC}CO_2$ extraction can obtain excellent quality extracts that are very suitable for the food, functional nutrition, cosmetics, and pharmaceutical industries. In addition, because of the high penetration and diffusibility of $_{SC}CO_2$, it effectively promotes the penetration of the solvent through the plant substrate, thereby accelerating the desorption and release from the substrate of the analyte, which then diffuses into the solvent, thus shortening the extraction time [11–13]. Therefore, $_{SC}CO_2$ extraction meets the requirements of economic efficiency in the industrialization process.

Based on the foregoing description, it is clear that $_{SC}CO_2$ is an excellent extraction solvent for nonpolar to low-polar components. Therefore, $_{SC}CO_2$ extraction has been widely used to extract volatile components from different substrates [14]. However, literature reports on the extraction of perilla oil with $_{SC}CO_2$ are scarce. In addition, the solubility of the analyte in $_{SC}CO_2$ is one of the important data for judging whether the $_{SC}CO_2$ extraction procedure is feasible and even good or bad in progress. Furthermore, the solubility data of the analyte are an indispensable parameter for subsequent pharmacokinetic experiments.

Although the diverse uses and pharmacological activities of perilla oil have been widely reported, data on its solubility in $_{SC}CO_2$ remain very limited. Therefore, this study primarily uses the $_{SC}CO_2$ dynamic extraction of perilla oil and carefully explores the effects of the CO_2 flow rate, temperature, and pressure on the yield to obtain the highest yield and best quality of the oil. Furthermore, three density-based correlation models with excellent accuracy are used to correlate the solubility of perilla oil obtained through experiments to expand the solubility data for subsequent pharmacokinetic experiments.

2. Materials and Methods

2.1. Raw Materials and Reagents

Dried *P. frutescens* leaves (the red-leaf form) were purchased from different local herbal shops (Kaohsiung, Taiwan) and then authenticated, triturated, sieved (W.S. Tyler, Mentor, OH, USA, 0.36 mm), and deposited [15]. Subsequently, the moisture content of the herb sample measured by volumetric Karl Fischer titration was 8.71% [16]. Helium (99.99%) and carbon dioxide (99.99%) were purchased from the Yun-Shan Gas Co. Ltd. (Tainan, Taiwan). Perillaldehyde, β-caryophyllene, (Z,E)-α-farnesene and limonene were obtained from Sigma Chemical Co. (St. Louis, MO, USA); n-hexane was bought from Merck Co. (Darmstadt, Germany).

2.2. Supercritical Carbon Dioxide ($_{SC}CO_2$) Extraction

A semibatch flow extraction procedure (Isco 260D, Lincoln, NE, USA) was used for $_{SC}CO_2$ extraction [17]. The extraction procedure was carried out by adding 20 g of plant sample (0.36 mm) into a stainless steel vessel (SS304, i.d. of 22 mm and length of 300 mm), which was later immersed in a large stainless steel water bath (SS304, length: 300 mm, width: 200 mm, height: 500 mm). After reaching the desired temperature and pressure, a static extraction stage (for 30 min) followed by a dynamic extraction stage (5–210 min) was carried out [18]. The oils were collected in two consecutive separators. The first separation tank is operated at 4 °C and 9 MPa, while the second separation tank is operated at 4 °C and 0.15 MPa.

2.3. Essential Oil Extraction by Hydrodistillation (HD)

In brief, 100 g of an herbal sample (0.36 mm) was placed in a 1.5 L distillation flask (3 holes), a certain amount of distilled water was added, and the device was connected with a Clevenger condenser. Subsequently, the distillation flask was immersed in a temperature-controlled water bath (Haake F3-K, Haake, Karlsruhe, Germany). After the desired temperature (100 °C) was obtained, a 4-h static stage extraction was performed for the HD procedure. The essential oil was further separated by the action of gravity. Anhydrous sodium sulfate was used to dry the obtained oils [19,20].

2.4. Gas Chromatographic (GC) Analysis

GC analyses of the essential oils were performed using a GC/flame ionization detector (FID) system (Shimadzu, model CG-14A, Kyoto, Japan) equipped with a DB-5 silica capillary column (30 m $\times$ 0.25 mm $\times$ 0.25 μm, J&W Scientific, Folsom, CA, USA) [21]. The quantities of the four main constituents, limonene, perillaldehyde, β-caryophyllene, and (Z,E)-α-farnesene were evaluated by comparing their peak areas to those of the calibration curves of the standards of constituents.

2.5. Statistical Analysis

All yields are estimated on the basis of plant dry weight, which is expressed using the average and standard deviation (SD) of three experimental results. The SD was calculated as follows:

$$SD = \sqrt{\frac{\sum\limits_{i=1}^{n} \left(y_{e,i} - y_m\right)^2}{n-1}} \tag{1}$$

where $y_{e,i}$ is the experimental value, y_m is the mean value, and n is the number of experimental runs [22].

To evaluate correlations in the applied models, the two objective functions average absolute relative deviation ($AARD(\%)$) and coefficient of determination (R^2) were determined using the predicted and experimental values. These parameters were calculated using Equations (2) and (3).

$$AARD(\%) = \frac{100\%}{n} \sum_{i=1}^{n} \left| \frac{y_{p,i} - y_{e,i}}{y_{e,i}} \right| \tag{2}$$

$$R^2 = 1 - \frac{\sum\limits_{i=1}^{n} \left(y_{e,i} - y_{p,i}\right)^2}{\sum\limits_{i=1}^{n} \left(y_{e,i} - y_m\right)^2} \tag{3}$$

where $y_{p,i}$ is the predicted value corresponding to point i.

3. Results and Discussion

3.1. Essential Oils Obtained by HD

Hydrodistillation (HD) and steam distillation (STD) are well-known standard procedures for extracting essential oils from natural sources. Therefore, to evaluate the performance of the $_{SC}CO_2$ extraction, this study first used the HD procedure for 4 h to extract the essential oil from *P. frutescens* leaves. The obtained essential oil has a pale yellow color and a strong fragrance. The yields of the essential oil and its four main components are shown in Table 1. The yields of essential oils and individual components were expressed in terms of the mass percent of the essential oil per gram of dry plant (%, g of oil/g of dry plant) and the mass percent of each component per gram of essential oil (%, g of component/g of oil), respectively.

Table 1. Comparison of the extraction conditions and yields obtained by hydrodistillation (HD) and supercritical carbon dioxide ($_{SC}CO_2$) extraction.

	HD	$_{SC}CO_2$ Extraction
Sample of *P. frutescens* leaves	P1	P1
Mean particle size (mm)	0.36	0.36
Plant weight (g)	100	20
Static extraction time (min)	—	30
Dynamic time (min)	—	170
Extraction time (min)	240	200
Extraction temperature (°C)	100	55
Extraction pressure (MPa)	—	33.0
CO_2 flow rate (g/min)	—	0.37
Yields		
oil (%, w/w) [1]	1.02 ± 0.02	1.33 ± 0.04
limonene (%, w/w) [2]	10.59 ± 0.50	11.81 ± 0.45
perillaldehyde (%, w/w) [2]	39.07 ± 1.62	40.52 ± 1.50
β-caryophyllene (%, w/w) [2]	9.14 ± 0.33	9.57 ± 0.36
(Z,E)-α-farnesene (%, w/w) [2]	4.95 ± 0.21	5.30 ± 0.20

[1]: Values are written as the mean $\pm$ SD (g of oil/g of dry plant weight) of the extracted oils.
[2]: Values are written as the mean $\pm$ SD (g of constituent/g of oil) of four replications.

3.2. Influence of the CO_2 Flow Rate

The extraction kinetic curve of the natural solid substratum using the $_{SC}CO_2$ dynamic procedure is usually called the overall extraction curve (OEC), which is often expressed as a graph of extraction yield versus extraction time or the mass of spent CO_2 for the extracting conditions (T, P, CO_2 flow rate, and cosolvent) [23]. The OEC not only predicts the extraction capacity of the procedure but also indicates the composition and physicochemical and biological characteristics of the extract. Furthermore, based on the experimental data of the OEC, a mathematical model of the extraction procedure can be derived to establish the parameters required by the extraction procedure, which can then be used as the basis for establishing optimized industrial procedures. Experimental OEC data fitted to a spline using two straight lines can usually be clearly divided into three stages: the constant extraction rate (CER), decreasing extraction rate and diffusion period [24–26]. Consequently, according to the kinetic parameters obtained in the CER period, such as the duration, mass transfer rate, and yield, the analyte concentration in the solvent phase at the vessel outlet (Y_{CER}) is further calculated. At a certain temperature and pressure and the most appropriate CO_2 flow rate, the Y_{CER} value will approach the maximum value (Y_{CER} *), which can be considered the theoretical solubility of the analyte in $_{SC}CO_2$. The proper CO_2 flow rate have to be sufficiently low to guarantee that the $_{SC}CO_2$ is saturated with solute at the outlet of the vessel, but it cannot restrict the mass transfer of the extraction process. Therefore, the CO_2 flow rate is one of the most crucial factors for determining the solubility of the solute in the supercritical solvent phase via the $_{SC}CO_2$ dynamic extraction method.

To evaluate the influence of CO_2 flow rate on the oil yield, $_{SC}CO_2$ extraction was performed at a static stage of 30 min followed by a dynamic stage of 5–270 min at a mean particle size of 0.36 mm [27]. To establish the OEC data, the extracts were collected at equal intervals of 5–10 min, and qualitative and quantitative analyses were further performed using GC analysis. The OECs of volatile oils using $_{SC}CO_2$ dynamic extraction at a serial flow rates were expressed as the oils/dry plant mass ratio (g/g, %) as a function of the CO_2/dry plant mass ratio (Figure 1). Then, the OECs obtained at different CO_2 flow rates were fitted using two straight lines, and the Y_{CER} value obtained at each flow rate in the CER period (first straight line) was therefore generated, as shown in Figure 2.

Increasing the CO_2 flow rate (0.09 to 0.37 g/min) increased the contact area and collision opportunity frequency between the solvent and the plant sample, which in turn increased the value of Y_{CER} (Figure 2). Additionally, the greater the CO_2 flow rate is, the steeper the concentration gradient difference between the analyte and the $_{SC}CO_2$ is, which

promotes the diffusion and mass transfer of the analyte and thereby enhances the value of Y_{CER}. However, if the CO_2 flow rate is too high (0.37 to 0.76 g/min), because of the declined extent of saturation of the supercritical solvent at higher flow rates, the value of Y_{CER} begins to decrease. Using $_{SC}CO_2$ extraction, a flow rate of 0.37 g/min generated the maximum value of Y_{CER} (Y_{CER}*) and was therefore determined as an appropriate CO_2 flow rate for evaluating the theoretical solubility of volatile oil in $_{SC}CO_2$.
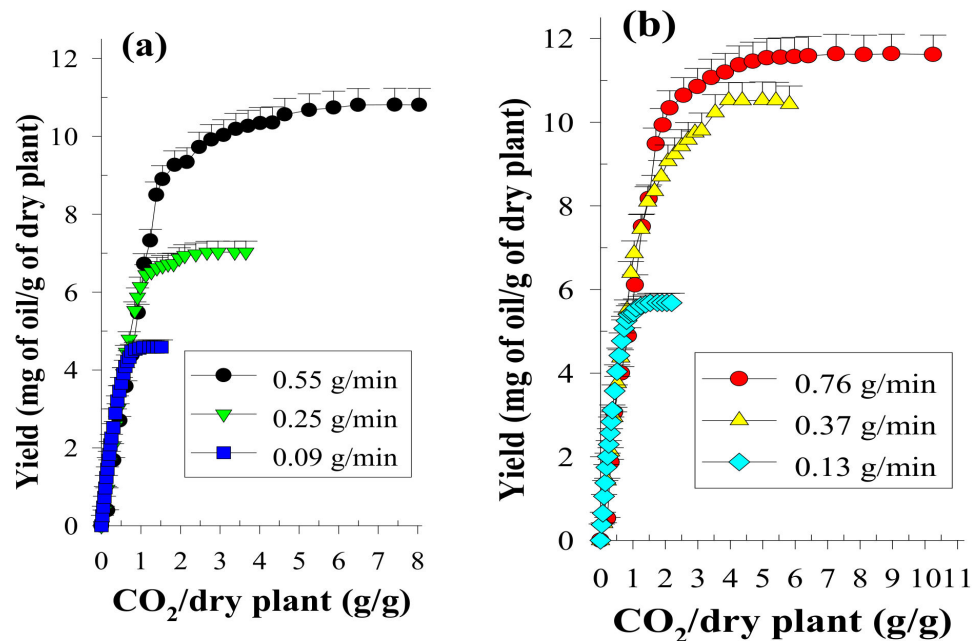

Figure 1. Overall extraction curves at 32 °C, 33.0 MPa and various CO_2 flow rates (**a**,**b**) for the $_{SC}CO_2$ extraction of volatile oils from *P. frutescens* leaves.
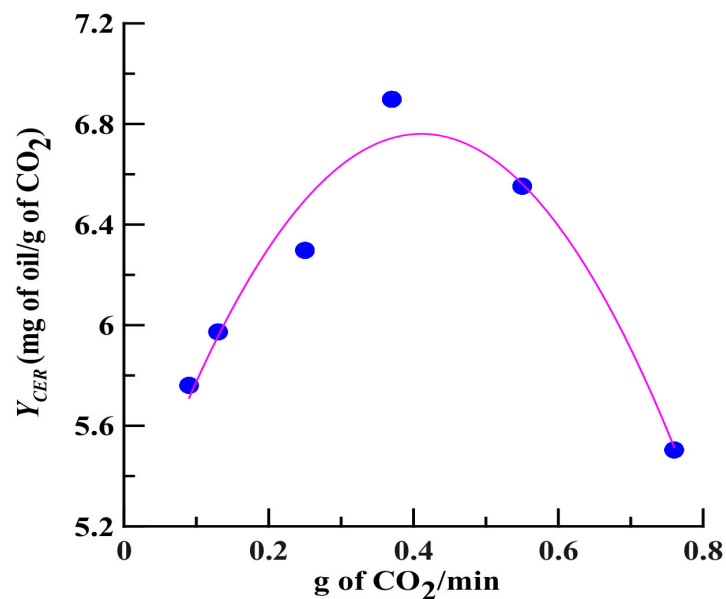

Figure 2. The effect of CO_2 flow rate on Y_{CER} (mg of oil/g of CO_2) value at 32 °C. The slope of the constant extraction rate (CER) period (a straight line) is defined as the Y_{CER} value, which is obtained by dividing the yield by the solvent/plant weight ratio. If the solvent is saturated with the solute, YCER should be maximized; this value is called the theoretical solubility (Y_{CER}*).

3.3. Influences of Temperature and Pressure

Pressure and temperature are the most important factors for the performance and selectivity of $_{SC}CO_2$ extraction, and this importance has been verified for different natural species [28]. To estimate the effects of both factors on the oil yields, $_{SC}CO_2$ extraction was conducted at pressures ranging from 10.5 to 33.0 MPa and temperatures ranging from 32 °C to 55 °C, while other conditions were kept fixed as mentioned above.

Figure 3 indicates that when the pressure increases from 10.5 MPa to 33.0 MPa, the yield of volatile oil increases substantially. This result is due to the increase in the density of the supercritical CO_2 with the increase in pressure, so the solubility of the oil in the supercritical solvent increases, enhancing the yield of oil [29,30]. However, at a pressure of 33.0 MPa, the increase in the oil yield was smaller, which may be due to the decrease in mass transfer and diffusion parameters as the pressure increased.
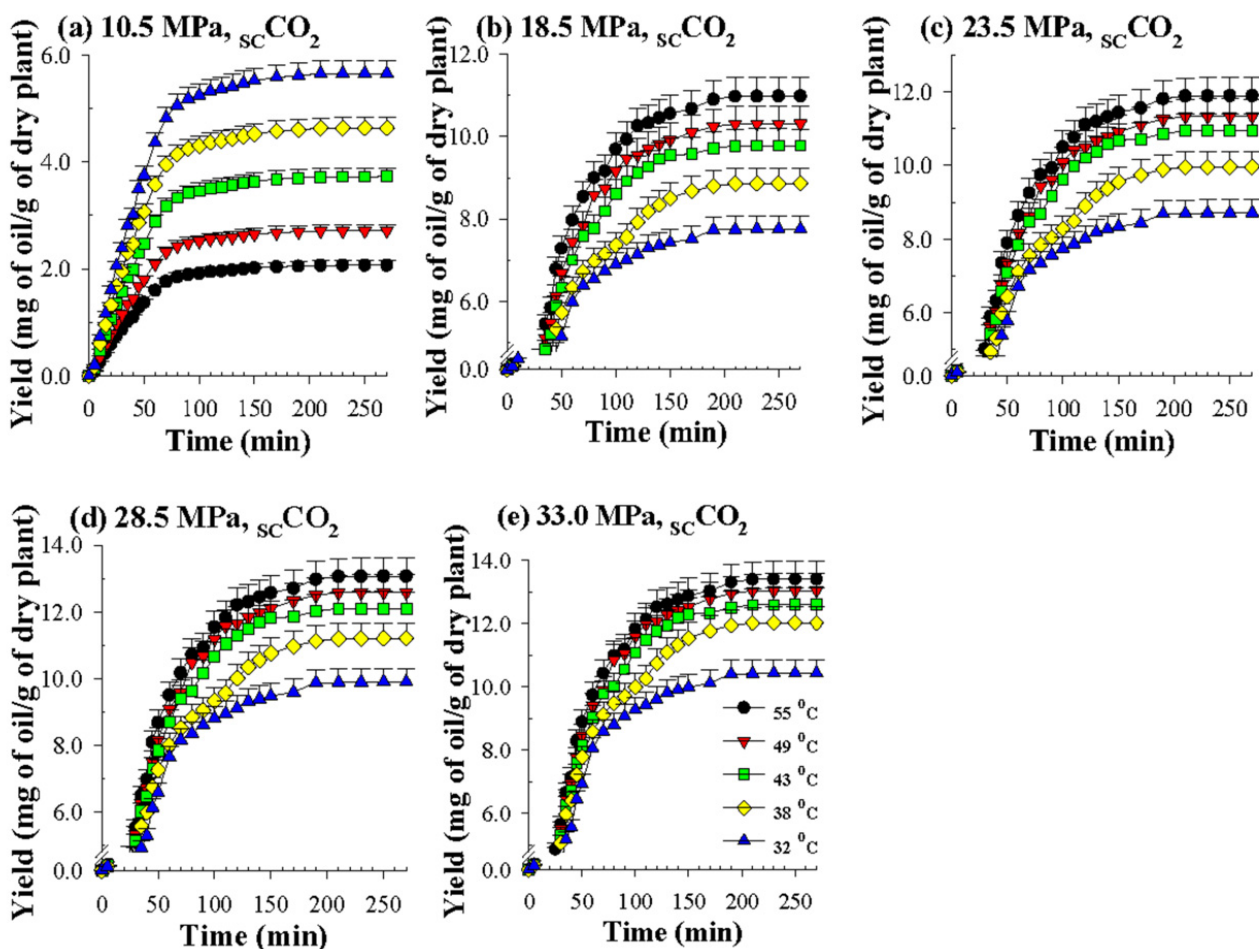

Figure 3. Overall extraction curves for $_{SC}CO_2$ dynamic extraction of volatile oils from *P. frutescens* leaves at various temperatures and pressures (**a**–**e**) and a CO_2 flow rate of 0.37 g/min.

As shown in Figure 3, the effect of temperature obviously has two opposing trends on the yields obtained by $_{SC}CO_2$ extraction at different pressures. Under the lower pressure of 10.5 MPa (Figure 3a), because it is closer to the critical pressure of CO_2 (7.39 MPa), when the extraction temperature increases from 32 °C to 55 °C, the density of supercritical CO_2 drops substantially, so the $_{SC}CO_2$ extraction capacity is reduced. However, under the four higher pressures (18.5, 23.5, 28.5, and 33.0 MPa) (Figure 3b–e), the extraction temperature obviously increases (32 °C to 55 °C), which is conducive to an increase in the extraction yield.

Although the increase in temperature causes the density of supercritical CO_2 to decrease, the vapor pressure, diffusion coefficient, and mass transfer coefficient of the

solute and solvent all increase with the temperature. The driving forces of these two different trends compete with each other; that is, the rise in the latter driving force offsets the fall in the former driving force, which benefits the improvement in the extraction capacity of $_{SC}CO_2$. The competing effects of the two apparently contradictory driving forces caused by the extraction temperature result in a crossover trend when $_{SC}CO_2$ dynamically extracts the perilla oil [31]. Similar to this phenomenon, it has also been observed that $_{SC}CO_2$ dynamically extracts different analytes, such as rice bran oil [31], crude oil [32] and coenzyme Q10 [33].

3.4. Characterization of Oils Obtained by $_{SC}CO_2$ Extraction and HD

As indicated in Table 1, the yields of oil and the main volatile components obtained by $_{SC}CO_2$ extraction for 200 min at 33.0 MPa and 55 °C were obviously higher than those of the HD procedure. The yield of volatile oils was 23.9% higher when acquired by $_{SC}CO_2$ extraction instead of HD. In addition, the contents of perillaldehyde, limonene, caryophyllene and (Z,E)-α-farnesene were approximately 1.02-, 1.12-, 1.05-, and 1.07-fold higher, respectively, when acquired by the $_{SC}CO_2$ procedure instead of HD extraction. In addition, the extracts obtained by $_{SC}CO_2$ extraction are stronger and deeper than those obtained by HD in terms of aroma and color. Therefore, it is inferred that $_{SC}CO_2$ extraction can obtain higher quality perilla oil than the HD procedure. Furthermore, the $_{SC}CO_2$ procedure reduced the time required (1.2-fold) and the operating temperature (45 °C). Therefore, these advantages of the $_{SC}CO_2$ procedure enable it to meet the green requirements.

3.5. Theoretical Solubility of Volatile Oils and Models

The OECs in Figure 3 obtained by $_{SC}CO_2$ dynamic extraction at different pressures and temperatures were further fitted to a spline using two straight lines. The slope of the first straight line (CER period) was used to calculate the theoretical solubility of volatile oil in supercritical CO_2, and the results are shown in Table 2. At all five extraction temperatures, the theoretical solubility increased substantially with pressure because of the increase in the supercritical CO_2 density. This result is similar to those of most studies using $_{SC}CO_2$ dynamic extraction [33,34].

However, when examining the influence of temperature on the theoretical solubility of oils in supercritical CO_2, the phenomenon of retrograde solubility in the supercritical solvent was inspected at 10.5 MPa (Table 2), where an increase in temperature leads to a decrease in the theoretical solubility under a pressure below that of the crossover zone, and at a pressure higher than that of this zone, the theoretical solubility of oils increases with temperature (32 °C to 55 °C). When $_{SC}CO_2$ is used to extract different analytes dynamically, retrograde solubility behavior is often observed [33,35].

The Chrastil [36] model is the most commonly used model for correlating solubility data and describes the relationship between the solubility of the volatile oil (Y^*_{oil}) and the density of supercritical CO_2 (ρ) as follows:

$$\ln(Y^*_{oil}) = a_0 + a_1 \ln(\rho) + \frac{a_2}{T} \tag{4}$$

where T is the extraction temperature (K); a_0, a_1 and a_2 are the model parameters; and a_2 is further denoted as

$$a_2 = \frac{-\Delta H_T}{R} \tag{5}$$

where ΔH_T is the total heat of the reaction or solution, and R is the universal gas constant (8.314 J/mol K).

Additionally, two models frequently utilized to correlate experimental data were proposed by Bartle [37] and Kumar and Johnston (K–J) [38]. The common features of these two models are simplicity and high accuracy. In the Bartle model, the correlation

between the experimental data and the density of supercritical CO_2 is demonstrated in a semi-logarithmic relationship.

$$\ln(Y^*_{oil}) = b_0 + b_1\rho + \frac{b_2}{T} \tag{6}$$

where b_0, b_1 and b_2 are the model parameters; and b_2 is further denoted as

$$b_2 = -\frac{\Delta H_T}{R} \tag{7}$$

Furthermore, in the Bartle model, in addition to the solubility data, density and temperature, the pressure parameter is added and is expressed in the following formula.

$$Ln\left(\frac{Y^*_{oil}P}{P_{ref}}\right) = c_0 + c_1(\rho - \rho_{ref}) + \frac{c_2}{T} \tag{8}$$

where c_0, c_1 and c_2 are the model parameters; P_{ref} is 0.1 MPa; ρ_{ref} is a reference density with a value of 700 g/L; and c_2 is further expressed as

$$c_2 = -\frac{\Delta H_{vap}}{R} \tag{9}$$

Table 2. Solubility data for the *P. frutescens* oils obtained by dynamic $_{SC}CO_2$ extraction.

T (°C)	P (MPa)	ρ (kg/m^3) [1]	$Y^*_{oil} \times 10^3$ (g oil/g CO$_2$) [2]
32	10.5	760.051	3.787 ± 0.152
	18.5	867.666	5.199 ± 0.20
	23.5	904.672	5.835 ± 0.234
	28.5	933.114	6.625 ± 0.265
	33.0	953.445	6.898 ± 0.276
38	10.5	667.094	3.105 ± 0.124
	18.5	834.302	5.783 ± 0.232
	23.5	877.501	6.496 ± 0.260
	28.5	909.376	7.308 ± 0.292
	33.0	931.632	8.065 ± 0.321
43	10.5	578.482	2.496 ± 0.101
	18.5	804.654	6.389 ± 0.256
	23.5	854.039	7.145 ± 0.287
	28.5	889.141	7.904 ± 0.319
	33.0	913.159	8.506 ± 0.343
49	10.5	441.899	1.818 ± 0.073
	18.5	766.348	6.742 ± 0.269
	23.5	824.725	7.409 ± 0.296
	28.5	864.279	8.227 ± 0.334
	33.0	890.625	8.853 ± 0.355
55	10.5	361.884	1.385 ± 0.055
	18.5	725.117	7.358 ± 0.296
	23.5	794.638	7.970 ± 0.321
	28.5	838.944	8.759 ± 0.352
	33.0	867.733	8.971 ± 0.367

[1] ρ: density of the scCO$_2$.
[2] Y^*_{oil}: the theoretical solubility of volatile oil in scCO$_2$.

Then, the solubility data obtained by $_{SC}CO_2$ dynamic extraction at different temperatures and pressures (Table 2) was linearly regressed using Equations (4) (Chrastil model), (6) (K–J model) and (8) (Bartle model), as shown in Figures 4–6, respectively. The coefficient of determination (R^2) was high, in the range of 0.992–0.999, which means that the three models mentioned above were sufficiently accurate to illustrate the solubility of the oils in

supercritical CO_2. Furthermore, Equations (4), (6), and (8) were used to perform multiple linear regression on the solubility data of the volatile oil, according to which all parameters of the three models were obtained (Table 3). Table 3 shows that all *AARD*(%) were less than 3.3% (1.39–3.25%), which again means that these three models reliably and accurately describe the solubility of volatile oil in supercritical solvents. In addition, using the three parameter values of a_2, b_2, and c_2, the heat of the solution (ΔH_T), vaporization (ΔH_{vap}), and solvation (ΔH_{solv}) for the supercritical binary systems were further calculated using Equations (5), (7), and (9), respectively (Table 3). The ΔH_T values obtained from the Chrastil ($\Delta H_{T,C}$) and K–J ($\Delta H_{T,K-J}$) models were 22.87 and 25.23 kJ/mol, respectively, and the value of ΔH_{vap} obtained using the Bartle model was 39.08 kJ/mol. It shows that vaporization is an endothermic process for binary systems. Therefore, the value of ΔH_{solv} was further calculated using the following equation [39]:

$$\Delta H_{solv} = \frac{1}{2}(\Delta H_{T,C} + \Delta H_{T,K-J}) - \Delta H_{vap} \tag{10}$$

The thermodynamic parameters in Table 3 indicate that the value of ΔH_{solv} is -15.03 kJ/mol, which demonstrates that solvation is an exothermic process for the oil-supercritical CO_2 binary systems. The value of ΔH_{solv} is negative because ΔH_{vap} was higher than ΔH_T in the oil-supercritical binary systems.
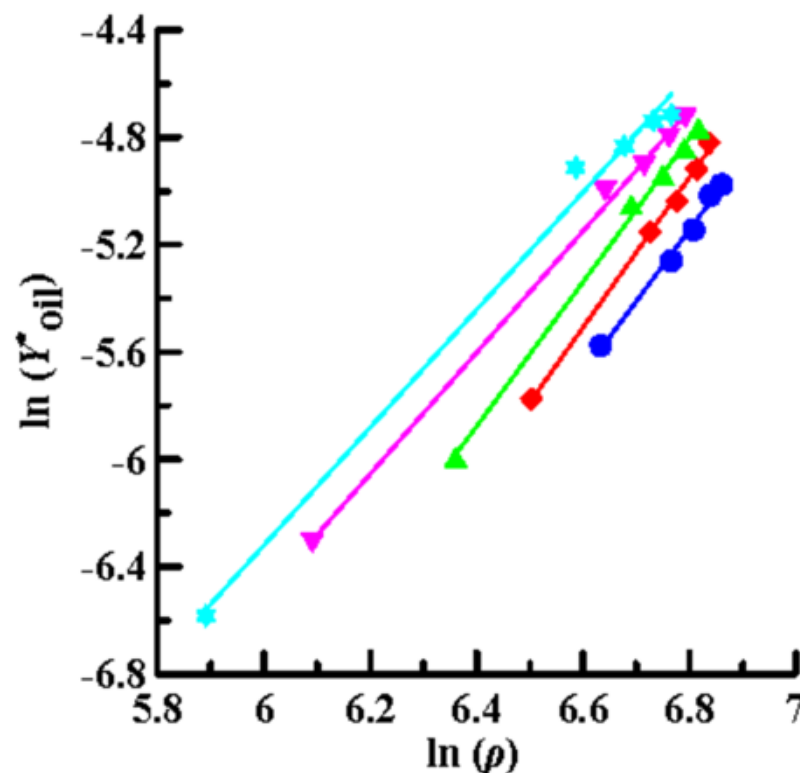

Figure 4. Plots of ln (Y^*_{oil}) versus ln (ρ) using the Chrastil model for oil extraction from *P. frutescens* leaves at various temperatures and pressures of 10.5–33.0 MPa. (●:32 °C; ◆: 38 °C; ▲: 43 °C; ▼: 49 °C; ★: 55 °C).
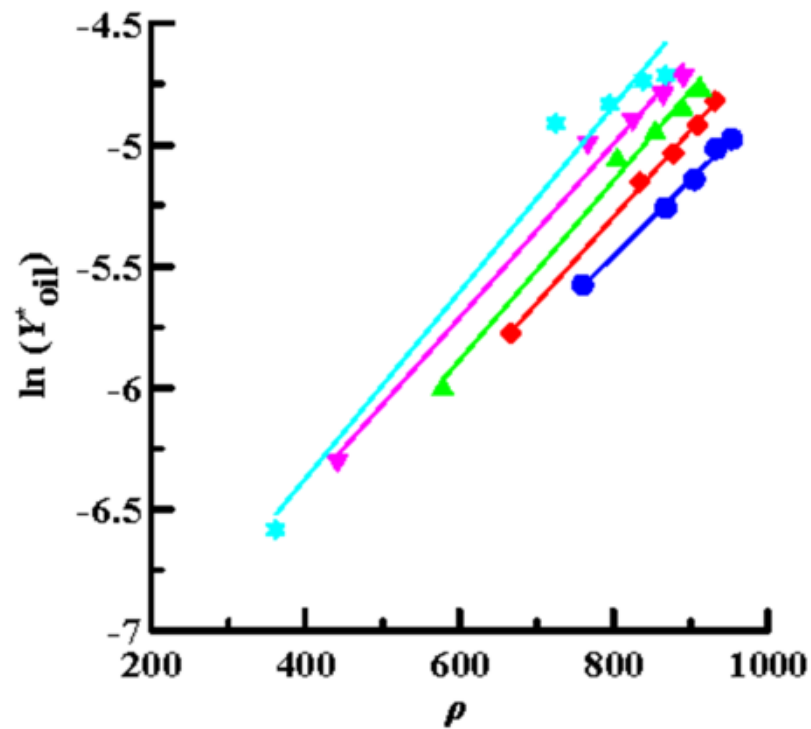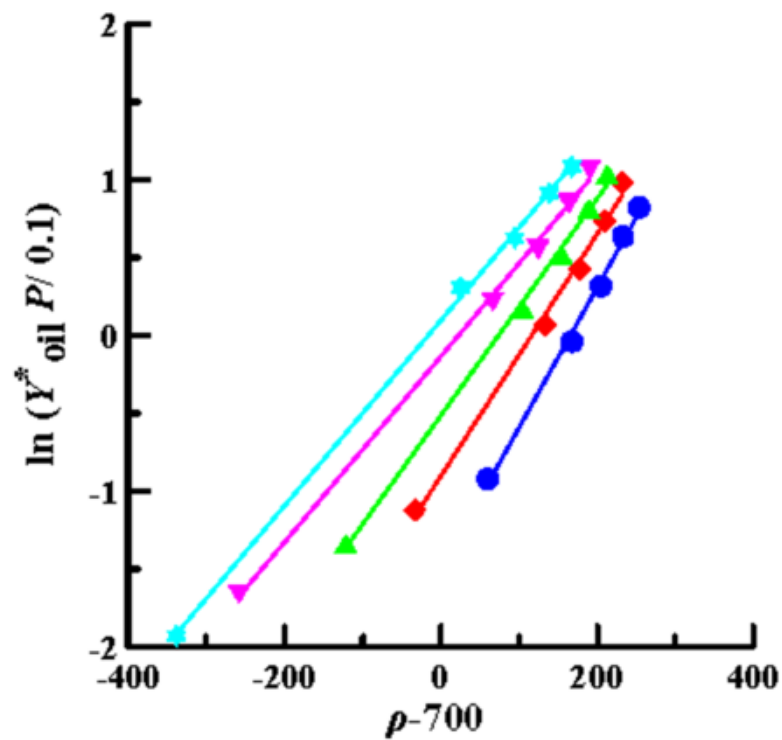
Figure 5. Plots of ln (Y^*_{oil}) versus ρ using the K–J model for oil extraction from *P. frutescens* leaves at various temperatures and pressures of 10.5–33.0 MPa. (●:32 °C; ◆: 38 °C; ▲: 43 °C; ▼: 49 °C; ★: 55 °C).

Figure 6. Plots of ln (Y^*_{oil} P/0.1) versus (ρ–700) using the Bartle model for oil extraction from *P. frutescens* leaves at various temperatures and pressures of 10.5–33.0 MPa. (●:32 °C; ◆: 38 °C; ▲: 43 °C; ▼: 49 °C; ★: 55°C).

Table 3. The fitted solubility parameters of three density-based models and the approximate heat of vaporization, total heat of solution and heat of solvation for *P. frutescens* oils obtained by dynamic $_{SC}CO_2$ extraction.

Model	n [4]	Parameters			$AARD$(%) [5]	Thermodynamic Parameters
		a_0:	a_1:	a_2:		$\Delta H_{T,C}$ (kJ/mol) [6]
1 [1]	25	–13.29	2.52	–2750.33	1.39	22.87
		b_0:	$10^3 b_1$:	b_2:		$\Delta H_{T,K-J}$ (kJ/mol) [7]
2 [2]	25	1.58	3.56	–3033.85	1.53	25.23
		c_0:	$10^3 c_1$:	c_2:		ΔH_{vap}(kJ/mol) [8]
3 [3]	25	14.19	6.97	–4701.20	3.25	39.08
						ΔH_{solv} (kJ/mol) [9]
						–15.03

[1] Chrastil model: $\ln(y^*_{oil}) = a_0 + a_1 \ln(\rho) + \frac{a_2}{T}$,

[2] K-J model: $\ln(y^*_{oil}) = b_0 + b_1 \rho + \frac{b_2}{T}$,

[3] Bartle model: $\ln(\frac{y^*_{oil} P}{P_{ref}}) = c_0 + c_1(\rho - \rho_{ref}) + \frac{c_2}{T}$, where y^* is the theoretical solubility; P is the pressure (MPa); P_{ref} is 0.1 MPa; ρ is the density of the scCO$_2$ (kg/m^3); ρ_{ref} is a reference density (700 kg/m^3); T is the temperature (K); a_0, a_1, a_2, b_0, b_1, b_2, c_0, c_1, and c_2 are the fitted parameters.
[4] Number of data points used in the correlation.

[5] Average absolute relative deviation. $AARD(\%) = \frac{100}{n} \sum\limits_{i=1}^{n} \left| \frac{y_{p,i} - y_{e,i}}{y_{e,i}} \right|$,

[6] Total heat of solution obtained from the Chrastil model, $\Delta H_{T, C} = -a_2 \times 8.314$ J/mol-K.
[7] Total heat of solution obtained from the K-J model, $\Delta H_{T, K-J} = -b_2 \times 8.314$ J/mol-K.
[8] Heat of vaporization obtained from the Bartle model, $\Delta H_{vap} = -c_2 \times 8.314$ J/mol-K.
[9] Heat of solvation, $\Delta H_{solv} = \frac{1}{2}(\Delta H_{T,C} + \Delta H_{T,K-J}) - \Delta H_{vap}$.

4. Conclusions

$_{SC}CO_2$ extraction and hydrodistillation (HD) extraction were used to separate the oils and the four main constituents in oils from *Perilla frutescens* leaves. $_{SC}CO_2$ extraction obtains higher yields of the oil and its four main components than the latter procedure, and uses milder operating conditions (duration time and temperature). Additionally, the theoretical solubilities of the oils obtained by the $_{SC}CO_2$ dynamic extraction at various temperatures and pressures were systematically evaluated, and retrograde solubility behavior was found in the oil-supercritical CO$_2$ binary systems. At a minimum experimental pressure (10.5 MPa), the density of CO$_2$ dominates the extraction capacity of $_{SC}CO_2$; therefore, this extraction procedure is suitable for lower temperatures. However, at higher pressures (18.5, 23.5, 28.5, and 33.0 MPa) the vapor pressure, mass transfer, and diffusion coefficients prevailed in the $_{SC}CO_2$ extraction; therefore, a higher temperature benefits the extraction process. Furthermore, the theoretical solubility was excellently correlated with three density-based models. Consequently, the heat of the solution, vaporization, and solvation for the oil-supercritical CO$_2$ binary systems were perfectly estimated. Because the heat of the solution and vaporization were both positive values, the entire $_{SC}CO_2$ extraction was an endothermic process. However, because the heat of solvation was negative, this step is an exothermic process.

Author Contributions: Conceptualization, M.-C.W.; data curation, D.-H.W. and Y.-C.Y.; formal analysis, D.-H.W. and Y.-C.Y.; investigation, M.-C.W., D.-H.W., and Y.-C.Y.; methodology, D.-H.W. and Y.-C.Y.; software, M.-C.W. and C.-S.W.; supervision, M.-C.W. and C.-S.W.; validation, M.-C.W., D.-H.W., and Y.-C.Y.; visualization, C.-S.W.; writing—original draft, Y.-C.Y.; writing—review and editing, M.-C.W., C.-S.W., and Y.-C.Y. All authors have read and agreed to the published version of the manuscript.

Institutional Review Board Statement: Not applicable.

References

1. Tabanca, N.; Demirci, B.; Ali, A.; Ali, Z.; Blythe, E.K.; Khan, I.A. Essential oils of green and red *Perilla frutescens* as potential sources of compounds for mosquito management. *Ind. Crops Prod.* **2015**, *65*, 36–44. [CrossRef]
2. Torri, L.; Bondioli, P.; Folegatti, L.; Rovellini, P.; Piochi, M.; Morini, G. Development of perilla seed oil and extra virgin olive oil blends for nutritional, oxidative stability and consumer acceptance improvements. *Food Chem.* **2019**, *286*, 584–591. [CrossRef] [PubMed]
3. Tian, J.; Zeng, X.B.; Zhang, S.; Wang, Y.Z.; Zhang, P.; Lu, A.J.; Peng, X. Regional variation in components and antioxidant and antifungal activities of *Perilla frutescens* essential oils in China. *Ind. Crops Prod.* **2014**, *59*, 69–79. [CrossRef]
4. Park, S.H.; Paek, J.H.; Shin, D.; Lee, J.Y.; Lim, S.S.; Kang, Y.H. Purple perilla extracts with α-asarone enhance cholesterol efflux from oxidized LDL-exposed macrophages. *Int. J. Mol. Med.* **2015**, *35*, 957–965. [CrossRef] [PubMed]
5. Yang, Y.C.; Wang, C.S.; Wei, M.C. Development and validation of an ultrasound-assisted supercritical carbondioxide procedure for the production of essential oils from *Perilla frutescens*. *LWT Food Sci. Technol.* **2020**, *128*, 109503. [CrossRef]
6. Chang, X.L.; Zhao, Z.L.; Li, X.L.; Xu, H.; Sun, Y.; Wang, W.H. Extraction and advanced adsorbents for the separation of perillaldehyde from *Perilla frutescens* (L.) Britton var. crispa f. viridis leaves. *Food Sci. Technol. Res.* **2014**, *20*, 189–199. [CrossRef]
7. You, C.X.; Wang, Y.; Zhang, W.J.; Yang, K.; Wu, Y.; Geng, Z.F.; Chen, H.P.; Jiang, H.Y.; Du, S.S.; Deng, Z.W.; et al. Chemical constituents and biological activities of the purple Perilla essential oil against *Lasioderma serricorne*. *Ind. Crops Prod.* **2014**, *61*, 331–337. [CrossRef]
8. Ahmed, H.M.; Tavaszi-Sarosi, S. Identification and quantification of essential oil content and composition, total polyphenols and antioxidant capacity of *Perilla frutescens* (L.) Britt. *Food Chem.* **2019**, *275*, 730–738. [CrossRef]
9. Chen, F.; Liu, S.; Zhao, Z.; Gao, W.; Ma, Y.; Wang, X.; Yan, S.; Luo, D. Ultrasound pre-treatment combined with microwave-assisted hydrodistillation of essential oils from *Perilla frutescens* (L.) Britt. leaves and its chemical composition and biological activity. *Ind. Crops Prod.* **2020**, *143*, 111908. [CrossRef]
10. Yang, Y.C.; Wang, C.S.; Wei, M.C. Insights into the major phenolic acids in *Perilla frutescens* obtained by a sustainable procedure. *J. Ind. Eng. Chem.* **2021**. In Press. [CrossRef]
11. Szydłowska-Czerniak, A.; Tułodziecka, A.; Karlovits, G.; Szłyk, E. Optimisation of ultrasound-assisted extraction of natural antioxidants from mustard seed cultivars. *J. Sci. Food Agric.* **2015**, *95*, 1445–1453. [CrossRef] [PubMed]
12. El Marsni, Z.; Torres, A.; Varela, R.M.; Molinillo, J.M.; Casas, L.; Mantell, C.; Martinez de la Ossa, E.J.; Macias, F. Isolation of bioactive compounds from sunflower leaves (*Helianthus annuus* L.) extracted with supercritical carbon dioxide. *J. Agric. Food Chem.* **2015**, *63*, 6410–6421. [CrossRef] [PubMed]
13. Sanjaya, R.E.; Tedjo, Y.Y.; Kurniawan, A.; Ju, Y.H.; Ayucitra, A.; Ismadj, S. Investigation on supercritical CO_2 extraction of phenolic-phytochemicals from an epiphytic plant tuber (*Myrmecodia pendans*). *J. CO_2 Util.* **2014**, *6*, 26–33. [CrossRef]
14. Yousefi, M.; Rahimi-Nasrabadi, M.; Pourmortazavi, S.M.; Wysokowski, M.; Jesionowski, T.; Ehrlich, H.; Mirsadeghi, S. Supercritical fluid extraction of essential oils. *Trends Anal. Chem.* **2019**, *118*, 182–193. [CrossRef]
15. Yang, Y.C.; Wei, M.C.; Lian, F.Y.; Huang, T.C. Simultaneous extraction and quantitation of oleanolic acid and ursolic acid from *Scutellaria barbata* D. Don by ultrasound-assisted extraction and high-performance liquid chromatography. *Chem. Eng. Comm.* **2014**, *201*, 482–500. [CrossRef]
16. Yang, Y.C.; Wei, M.C.; Hong, S.J. Ultrasound-assisted extraction and quantitation of oils from *Syzygium aromaticum* flower bud (clove) with supercritical carbon dioxide. *J. Chromatogr. A* **2014**, *1323*, 18–27. [CrossRef]
17. Yang, Y.C.; Wang, C.S.; Wei, M.C. Kinetics and mass transfer considerations for an ultrasound-assisted supercritical CO_2 procedure to produce extracts enriched in flavonoids from *Scutellaria barbata*. *J. CO_2 Util.* **2019**, *32*, 219–231. [CrossRef]
18. Yang, Y.C.; Wei, M.C. A combined procedure of ultrasound-assisted and supercritical carbon dioxide for extraction and quantitation oleanolic and ursolic acids from *Hedyotis corymbosa*. *Ind. Crops Prod.* **2016**, *79*, 7–17. [CrossRef]
19. Huang, B.K.; Lei, Y.L.; Tang, Y.H.; Zhang, J.C.; Qin, L.P.; Liu, J.A. Comparison of HS-SPME with hydrodistillation and SFE for the analysis of the volatile compounds of Zisu and Baisu, two varietal species of *Perilla frutescens* of Chinese origin. *Food Chem.* **2011**, *125*, 268–275. [CrossRef]

20. Liu, Y.; Wang, H.; Zhang, J. Comparison of MAHD with UAE and hydrodistillation for the analysis of volatile oil from four parts of *Perilla frutescens* cultivated in southern China. *Anal. Lett.* **2012**, *45*, 1894–1909. [CrossRef]

21. Wei, M.C.; Xiao, J.; Yang, Y.C. Extraction of α-humulene-enriched oil from clove by ultrasound-assisted supercritical carbon dioxide extraction and studies of its fictitious solubility. *Food Chem.* **2016**, *210*, 172–181. [CrossRef] [PubMed]

22. Yang, Y.C.; Wang, C.S.; Wei, M.C. Separation and quantification of bioactive flavonoids from *Scutellaria barbata* using a green procedure. *Food Bioprod. Process.* **2019**, *118*, 77–90. [CrossRef]

23. Wei, M.C.; Yang, Y.C. Kinetic studies for ultrasound-assisted supercritical carbon dioxide extraction of triterpenic acids from healthy tea ingredient *Hedyotis diffusa* and *Hedyotis corymbosa*. *Sep. Purif. Technol.* **2015**, *142*, 316–325. [CrossRef]

24. Yang, Y.C.; Wang, C.S.; Wei, M.C. A green approach for the extraction and characterization of oridonin and ursolic and oleanolic acids from *Rabdosia rubescens* and its kinetics behavior. *Food Chem.* **2020**, *319*, 126582. [CrossRef]

25. Ferreira, S.R.S.; Meireles, M.A.A. Modeling the supercritical fluid extraction of black pepper (*Piper nigrum* L.) essential oil. *J. Food Eng.* **2002**, *54*, 263–269. [CrossRef]

26. Santana, Á.L.; Queirós, L.D.; Martínez, J.; Macedo, G.A. Pressurized liquid- and supercritical fluid extraction of crude and waste seeds of guarana (*Paullinia cupana*): Obtaining of bioactive compounds and mathematical modeling. *Food Bioprod. Process.* **2019**, *117*, 194–202. [CrossRef]

27. Wei, M.C.; Hong, S.J.; Yang, Y.C. Isolation of triterpenic acid-rich extracts from *Hedyotis corymbosa* using ultrasound-assisted supercritical carbon dioxide extraction and determination of their fictitious solubilities. *J. Ind. Eng. Chem.* **2017**, *48*, 202–211. [CrossRef]

28. Yang, Y.C.; Wei, M.C. Development and characterization of a green procedure for apigenin extraction from *Scutellaria barbata* D. Don. *Food Chem.* **2018**, *252*, 381–389. [CrossRef]

29. Said, P.P.; Pradhan, R.C.; Rai, B.N. A green separation of *Lagenaria siceraria* seed oil. *Ind. Crops Prod.* **2014**, *52*, 796–800. [CrossRef]

30. Wei, M.C.; Yang, Y.C.; Hong, S.J. Determination of oleanolic and ursolic acids in *Hedyotis diffusa* using hyphenated ultrasound-assisted supercritical carbon dioxide extraction and chromatography. *Evid. Based Complement. Alternat. Med.* **2015**, *2015*, 450547. [CrossRef]

31. Tomita, K.; Machmudah, S.; Fukuzato, R.; Kanda, H.; Quitain, A.T.; Sasaki, M.; Goto, M. Extraction of rice bran oil by supercritical carbon dioxide and solubility consideration. *Sep. Purif. Technol.* **2014**, *12*, 5319–5325. [CrossRef]

32. Rudyk, S.; Spirov, P.; Tyrovolas, A. Effect of temperature on crude oil extraction by SC-CO$_2$ at 40–70 °C and 40–60 MPa. *J. CO$_2$ Util.* **2018**, *24*, 471–478. [CrossRef]

33. Couto, R.; Seifried, B.; Moquin, P.; Temellia, F. Coenzyme Q10 solubility in supercritical CO$_2$ using a dynamic system. *J. CO$_2$ Util.* **2018**, *24*, 315–320. [CrossRef]

34. Yang, Y.C.; Wei, M.C. Ethanol solution-modified supercritical carbon dioxide extraction of triterpenic acids from *Hedyotis corymbosa* with ultrasound assistance and determination of their solubilities. *Sep. Purif. Technol.* **2015**, *150*, 204–214. [CrossRef]

35. Wei, M.C.; Lin, P.H.; Hong, S.J.; Chen, J.M.; Yang, Y.C. Development of a green alternative procedure for simultaneous separation and quantification of clove oil and its major bioactive constituents. *ACS Sustain. Chem. Eng.* **2016**, *4*, 6491–6499. [CrossRef]

36. Chrastil, J. Solubility of solids and liquids in supercritical gases. *J. Phys. Chem.* **1982**, *86*, 3016–3021. [CrossRef]

37. Bartle, K.D.; Clifford, A.; Jafar, S.A.; Shilton, G.F. Solubilities of solids and liquids of low volatility in supercritical carbon dioxide. *J. Phys. Chem. Ref. Data* **1991**, *20*, 713–756. [CrossRef]

38. Kumar, S.K.; Johnston, K.P. Modeling the solubility of solids in supercritical fluids with density as the independent variable. *J. Supercrit. Fluids* **1988**, *1*, 15–22. [CrossRef]

39. Yang, Y.C.; Lin, P.H.; Wei, M.C. Production of oridonin-rich extracts from *Rabdosia rubescens* using hyphenated ultrasound-assisted supercritical carbon dioxide extraction. *J. Sci. Food Agric.* **2017**, *97*, 3323–3332. [CrossRef]